Quantitative Analyses of Carbonyl-Carbon-11-WAY-100635 Binding to Central 5-Hydroxytryptamine-1A Receptors in Man

Lars Farde, Hiroshi Ito, Carl-Gunnar Swahn, Victor W. Pike and Christer Halldin

Psychiatry Section, Department of Clinical Neuroscience, Karolinska Institutet, Stockholm, Sweden; and Chemistry and Engineering Group, Medical Research Council Cyclotron Unit, Imperial College School of Medicine, Hammersmith Hospital, London, United Kingdom

The serotonin 5-hydroxytryptamine-1A (5-HT_{1A}) receptor subtype is of central interest in research on the pathophysiology and treatment of psychiatric disorders. Carbonyl-^{11}C-WAY-100635 is a new radioligand that, in PET experiments, provides high-contrast delineation of brain regions that are rich in 5-HT_{1A} receptors. The aim of this PET study was to examine the prospects for quantitation of carbonyl-^{11}C-WAY-100635 binding to 5-HT_{1A} receptors in the human brain. **Methods:** A PET examination was performed in each of six healthy male subjects after intravenous injection of carbonyl-^{11}C-WAY-100635. Radioactive metabolites in plasma were determined with high-performance liquid chromatography. The metabolite-corrected arterial input function was used in a kinetic three-compartment analysis, and the cerebellum was used as reference region in linear graphical and transient equilibrium analyses. **Results:** The highest radioactivity concentration was observed in the neocortex and the raphe nuclei, whereas radioactivity was low in the cerebellum. The time–activity curves were well-described by a three-compartment model for all regions. Uptake in the cerebellum could not be described by a two-compartment model. The transient equilibrium and linear graphical analyses, which are both dependent on the cerebellum as the reference region, gave lower binding potential values than did the kinetic analysis. The metabolism was rapid, and the fraction of unchanged carbonyl-^{11}C-WAY-100635 was <10% 10 min after injection in all human subjects. The major radioactive metabolites were unidentified polar components. One metabolite comigrated with reference cyclohexanecarboxylic acid, and another comigrated with reference desmethyl-WAY-100635. **Conclusion:** The suitability of carbonyl-^{11}C-WAY-100635 for research on central 5-HT_{1A} receptors in neuropsychiatric disorders was supported by the observation that the high signals in the neocortex and raphe nuclei can be described using a kinetic analysis with a metabolite-corrected arterial input function. It cannot be excluded that kinetically distinguishable nonspecific binding or the formation of a metabolite that passes the blood–brain barrier may represent measurable components of the low radioactivity in the cerebellum. Simplified quantitative methods, using the relatively low radioactivity in the cerebellum as reference, should accordingly be applied with some caution until the biochemical nature of the radioactivity is better understood and the reliability of these approaches has been confirmed in larger samples.

Key Words: brain; human; 5-HT_{1A} receptors; serotonin; WAY-100635

J Nucl Med 1998; 39:1965–1971

The 5-hydroxytryptamine-1A (5-HT_{1A}) receptor is a serotonin (5-HT) receptor subtype of central interest in research on the pathophysiology and treatment of psychiatric disorders. Presynaptic 5-HT_{1A} receptors mediate inhibition of 5-HT release and are highly concentrated on cell bodies in the raphe nuclei. This autoreceptor has been given a key role in current hypotheses on the drug treatment of anxiety and depression (*1–3*). The high density of postsynaptic 5-HT_{1A} receptors in the neocortex is of particular interest in schizophrenia research because several laboratories have demonstrated elevated receptor binding in the neocortex of schizophrenic brains postmortem (*4,5*). Research on the functional role of 5HT_{1A} receptors in pharmacology and neuropsychiatric disorders has, however, been hampered by the lack of suitable radioligands for brain imaging of 5-HT_{1A} receptors in vivo.

WAY-100635 [N-(2-(4-(2-methoxyphenyl)-1-piperazinyl) ethyl)-*N*-(2-pyridyl)cyclohexanecarboxamide] is the first antagonist that binds with high affinity and selectivity to the 5-HT_{1A} receptor (*6,7*). Initially, WAY-100635 was labeled with ^{11}C ($t_{1/2}$ = 20.4 min) in the O-methyl position and explored as radioligand for PET studies in monkey (*8,9*) and man (*10*). More recently, WAY-100635 was labeled with ^{11}C in the carbonyl position (Fig. 1), a position that avoids formation of radioactive WAY-100634 and provides improved contrast in the human brain (*11*).

The anatomical distribution of [^{3}H-WAY-100635 binding has been described in detail using large-scale autoradiography on human hemispheric brain cryosections (*12*). High densities of 5-HT_{1A} receptors were found in the hippocampus, layers of the neocortex and the raphe nuclei, whereas the cerebellar cortex was virtually devoid of 5-HT_{1A} receptors. In a recent PET study on cynomolgus monkeys, the binding of carbonyl-^{11}C-WAY-100635 was markedly inhibited by pretreatment with unlabeled WAY-100635 and the reference ligands 8-hydroxy-N,N-dipropylaminotetralin (8-OH-DPAT), buspirone and pindolol (*13*). This inhibition confirms the specificity of carbonyl-^{11}C-WAY-100635 binding to 5-HT_{1A} receptors in vivo and indicates that the method has potential for determination of 5-HT_{1A} receptor occupancy during treatment with psychoactive drugs.

The aim of this PET study was to examine the prospects for quantitation of central carbonyl-^{11}C-WAY-100635 binding to 5-HT_{1A} receptors in the human brain. Six healthy men were recruited, and a metabolite-corrected arterial input function was used in kinetic compartment and linear graphical analyses.

MATERIALS AND METHODS

Subjects

The study was approved by the ethics committee of the Karolinska Hospital. Six men (age range 20–42 yr) participated after giving informed consent. They were healthy according to history, physical examination, psychiatric interview, blood and urine analyses and MRI of the brain. They did not use any medication.

Received Oct. 8, 1997; revision accepted Jan. 28, 1998.

For correspondence or reprints contact: Lars Farde, MD, PhD, Psychiatry Section, Karolinska Hospital, S-171 76 Stockholm, Sweden.

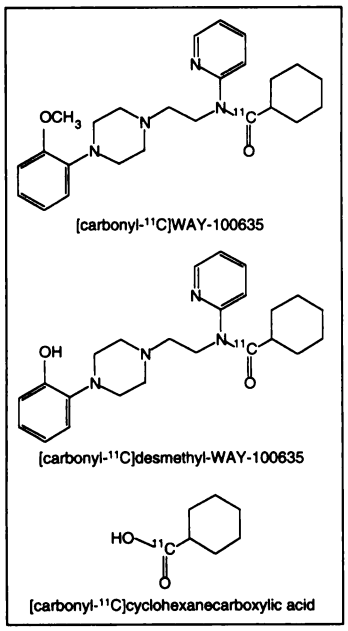

FIGURE 1. Chemical structure of carbonyl-^{11}C-WAY-100635 and two metabolites.

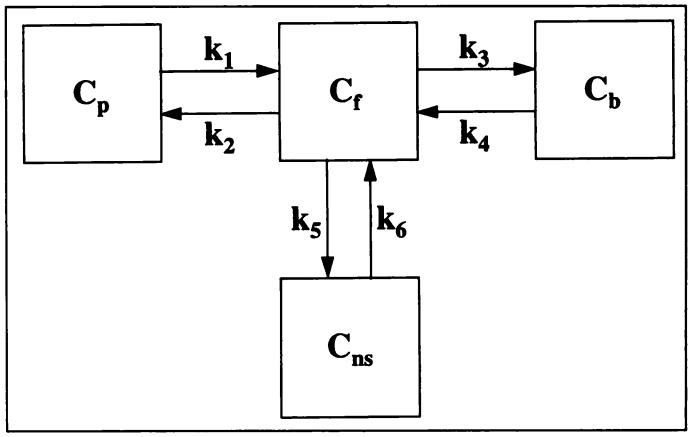

FIGURE 2. Four-compartment model.

Radiochemistry

Carbonyl-^{11}C-WAY-100635 was prepared by ^{11}C-acylation of WAY-100634 with carbonyl-^{11}C-cyclohexanecarbonyl chloride as described previously (*11,12*). The decay-corrected radiochemical yield of carbonyl-^{11}C-WAY-100635 from ^{11}C-cyclohexanecarbonyl chloride was 30%–50%. The purification by reverse-phase high-performance liquid chromatography (HPLC) using methanol, 0.1 *M* ammonium formate and triethylamine (60:40:0.3, v/v) as mobile phase was performed with good separation between the product and the precursor, WAY-100634. The radiochemical purity of the final product was >99%.

MRI

The MRI system used was GE Signa (1.5 T). T2-weighted and proton density magnetic resonance images of the brain were obtained for all subjects. The positioning of the head and the series of sections were the same as those in the PET studies. A head fixation system with an individual plaster helmet was used both in the PET and MRI measurements to allow the same head positioning in the two imaging modalities (*14*).

PET Experimental Procedure

The PET system used was Siemens ECAT Exact HR, which was run in the three-dimensional mode. Acquisitions were done with the interplane septa retracted and a wide axial acceptance angle. The reconstructed volume was displayed as 47 sections with a center to center distance of 3.125 mm.

In each PET measurement, the subject was placed recumbent with his head in the PET system. A cannula was inserted into the left brachial artery and another cannula into the right antebrachial vein. A sterile physiological phosphate buffer (pH = 7.4) solution containing carbonyl-^{11}C-WAY-100635 (219–357 MBq) was injected intravenously as a bolus for 2 sec. The specific radioactivity was 700–2700 Ci/mmol (26–100 GBq/μmol) at time of injection.

Brain radioactivity was measured in a series of consecutive time frames for up to 63 min. The frame sequence consisted of three 1-min frames followed by four 3-min frames and eight 6-min frames.

Arterial Blood Sampling

To obtain the arterial input function, an automated blood sampling system was used during the first 5 min of each PET experiment, whereupon arterial blood samples were taken manually at the midpoint of each frame until the end of the measurement (*15*).

Determination of Radioactive Metabolites in Plasma

The fractions of plasma radioactivity corresponding to unchanged carbonyl-^{11}C-WAY-100635 and metabolites were determined as described recently (*9,16*). Arterial plasma samples (2 ml) were deproteinized with acetonitrile and analyzed by gradient HPLC on a reverse-phase column (Waters μ-Bondapak C18; 7.8 × 300 mm, 10 μm) eluted at 6 ml/min over 7.5 min with acetonitrile-0.01 *M* phosphoric acid, using a gradient of 25%–60% acetonitrile from 0 to 5.5 min and 60%–25% acetonitrile from 5.5 to 6.5 min. Two reference compounds, cyclohexanecarboxylic acid and desmethyl-WAY-100635, were used to provide retention times for possible labeled metabolites in plasma.

Regions of Interest

Regions of interest (ROIs) were drawn on the magnetic resonance images and transferred to the reconstructed PET images. ROIs were anatomically delineated for the cerebellar cortex, the raphe, the medial temporal lobe including the hippocampus, the lateral temporal cortex and the frontal cortex. The ROIs for the cerebellum and the cortical regions were drawn in three adjacent sections, and data were pooled, so that the average radioactivity concentration for the whole volume of interest was obtained. The ROI for the raphe was drawn in three sections. The frontal cortex was drawn at the level of the basal ganglia, whereas the temporal cortex and the raphe nuclei were drawn at the level of the hippocampus. To obtain regional time-activity curves, regional radioactivity was calculated for each frame, corrected for decay and plotted versus time.

Kinetic Analyses

The data were analyzed using compartment models. The general configuration is a conventional four-compartment model (Fig. 2). The four compartments correspond to the radioactivity concentrations of unchanged radioligand in plasma (C_p), free (unbound) radioligand in brain (C_f), nonspecifically bound radioligand in brain (C_{ns}) and radioligand specifically bound to receptors (C_b). All concentrations are in units of nCi/ml.

A common assumption is that the two compartments C_f and C_{ns} equilibrate rapidly to form one effective compartment (*17*), corresponding to nondisplaceable radioligand in brain (C_n). The model simplified in this manner, with three compartments and four first-order rate constants, K_1, k_2, k_3 and k_4 (*17–19*), was used to describe the time-activity curves for carbonyl-^{11}C-WAY-100635 binding in the neocortex and the raphe nuclei. The rate constants K_1 and k_2 correspond to the influx and efflux rates for radioligand diffusion through the blood-brain barrier, respectively. The rate constants k_3 and k_4 correspond to the rates for radioligand transfer

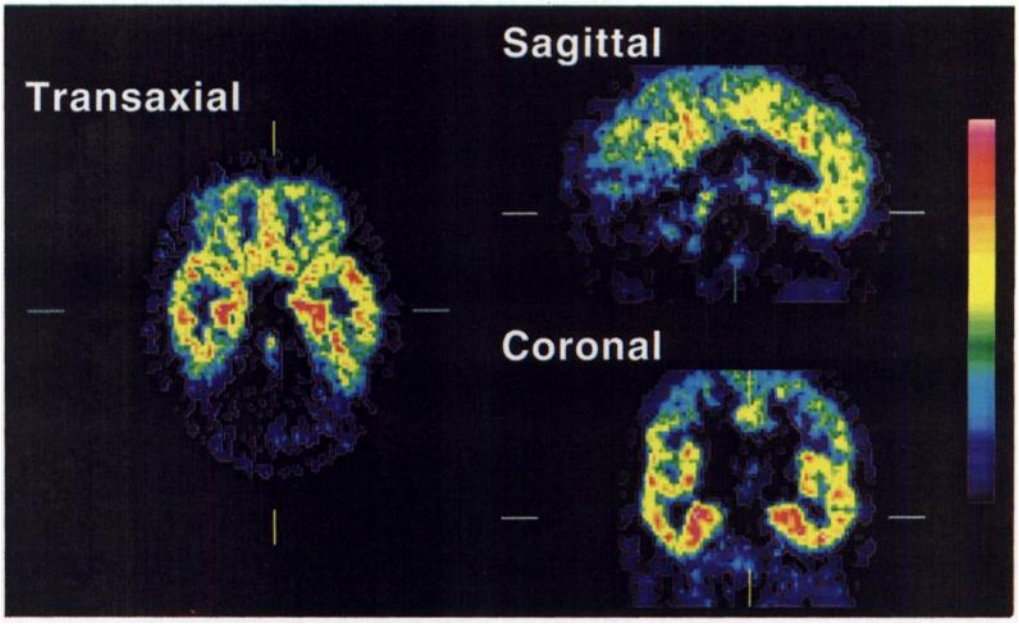

FIGURE 3. PET images of Subject B in three projections, obtained by summation of frames acquired from 33 to 63 min after intravenous injection of carbonyl-^{11}C-WAY-100635. Subject's right is on left in transaxial and coronal projection. Anterior is on right in sagittal projection.

between the compartments for nondisplaceable and specific radioligand binding to receptors, respectively. It was assumed that all compartments are homogeneous in concentration. The concentration in plasma (C_p) was not corrected for plasma protein binding. On the basis of this model, the following differential equations can be expressed:

$$dC_n(t)/dt = K_1 \cdot C_p(t) - (k_2 + k_3) \cdot C_n(t) + k_4 \cdot C_b(t), \quad \text{Eq. 1}$$

$$dC_b(t)/dt = k_3 \cdot C_n(t) - k_4 \cdot C_b(t) \quad \text{Eq. 2}$$

and

$$C_t(t) = C_n(t) + C_b(t), \quad \text{Eq. 3}$$

where $C_t(t)$ is the radioactivity concentration in brain, as measured by PET.

The four rate constants were determined by curve fitting in a least squares sense to a nonlinear solution (*20*). The time curve for the radioactivity of unchanged carbonyl-^{11}C-WAY-100635 in arterial plasma was used as input function.

Cerebellum as Reference Region. The cerebellum has been suggested as a reference region because this region is almost devoid of 5-HT_{1A} receptors in vitro (*12*). A two-compartment model with two rate constants should be sufficient to describe the time-activity curves in a region devoid of specific binding sites, which do not have the specific binding compartment (C_b). This common assumption of rapid equilibration between the two compartments C_f and C_{ns} was examined by using both a two-compartment and a three-compartment model with the rate constants K_1, k_2, k_5 and k_6 to describe the time-activity curves for carbonyl-^{11}C-WAY-100635 binding (*13*). To compare the two models, three statistical methods were used: the Akaike information criterion (*21*), the Schwarz criterion (*22*) and F statistics (*23*).

Distribution Volume. Carbonyl-^{11}C-WAY-100635 binding was also expressed using the concept of the "total distribution volume," V_t, which is defined by the following equation (*24*):

$$V_t = (K_1/k_2) \cdot (1 + k_3/k_4). \quad \text{Eq. 4}$$

To calculate V_t, the rate constants obtained from the three-compartment model analysis were entered into Equation 4.

Binding Potential. The three-compartment model analysis is based on the use of a radioligand with high specific radioactivity. Under such conditions, the receptor density (B_{max}) and affinity (K_d) cannot be differentiated (*18*). The B_{max}-to-K_d ratio corresponds to the k_3-to-k_4 ratio in the kinetic analysis or the $C_b(t)$-to-$C_n(t)$ ratio in the transient equilibrium analysis (described below) (*13*) and is often referred to as the binding potential (BP) (*18*).

Linear Graphical Analysis. Carbonyl-^{11}C-WAY-100635 binding was also analyzed using a linear graphical analysis for reversible ligand binding to receptors (*25*). The regional distribution volumes (DV^{Logan}) were determined from the slope of the linear plots obtained using the radioactivity of unchanged carbonyl-^{11}C-WAY-100635 in arterial plasma as an input function. The BP is given by the equation:

$$DV_{ROI}/DV_{cerebellum} - 1 = BP. \quad \text{Eq. 5}$$

Transient Equilibrium. The condition of transient equilibrium is theoretically defined as occurring when the derivative for $C_b(t)$ is zero (*13*). Because the cerebellum is a brain structure virtually devoid of 5-HT_{1A} receptors, the radioactivity concentration in the cerebellum was used as an estimate for $C_n(t)$. The fitted curves obtained in the kinetic analysis for $C_t(t)$ and the cerebellum, $C_{cerebellum}(t)$, were used to calculate $C_b(t)$.

Cerebral Blood Volume. Two approaches were applied to correct for the effect of cerebral blood volume (CBV). The first was to exclude the first four frames (0–60 sec) of the regional time-activity curves (*26*). The second was to use reference values for regional CBV (*27*) and the curve for measured radioactivity in arterial whole blood. The radioactivity was calculated in this manner for CBV for cross-validation purposes and then subtracted from the regional time-activity curves before the kinetic analyses. The rate constants obtained by the two approaches were compared.

RESULTS

After intravenous injection of carbonyl-^{11}C-WAY-100635, the radioactivity appeared rapidly in brain (Fig. 3). Radioactivity in the neocortex and the raphe was high, whereas that in the cerebellum was at a low level. The time courses for regional brain radioactivity are shown in Figure 4A. Among the neocortical regions, radioactivity was highest in the medial temporal cortex, a region that includes the hippocampus.

The time-activity curves for the neocortical regions, the raphe nuclei and the cerebellum were well described by the three-compartment model (Fig. 5). The rate constants are given in Table 1. The two approaches that were applied to correct for the effect of CBV gave almost identical results in the kinetic

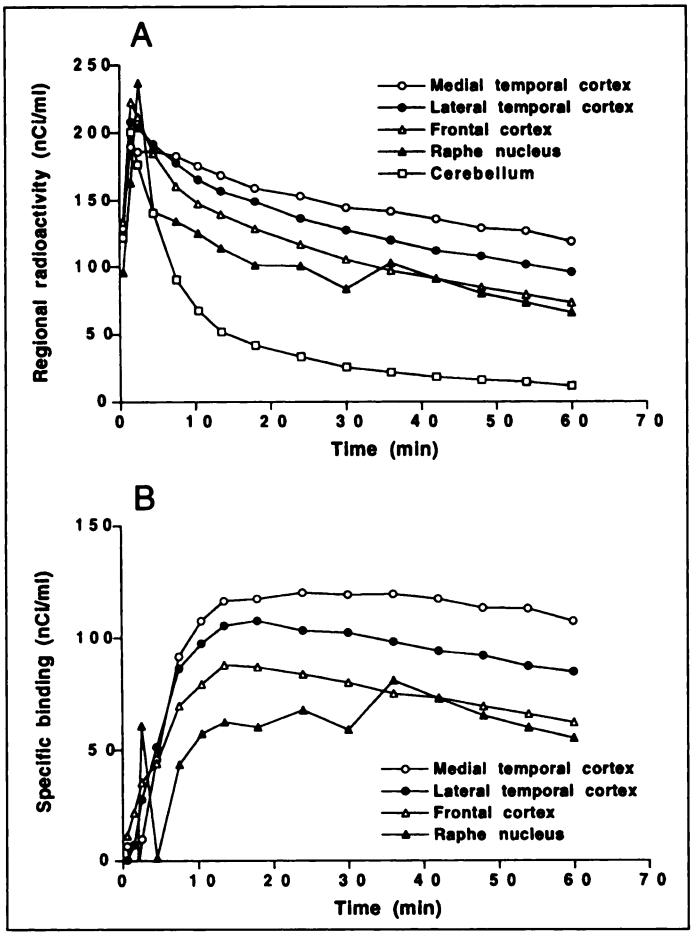

FIGURE 4. (A) Time curves for regional brain radioactivity after intravenous injection of 357 MBq of carbonyl-^{11}C-WAY-100635 in Subject B. (B) Time curves for specific carbonyl-^{11}C-WAY-100635 binding.

analysis (data not shown). The BPs (k_3/k_4) for the neocortical regions and the raphe were 7.8–14.3 (Table 2).

The uptake curve for the cerebellum was, in contrast, not adequately described by the two-compartment model (Fig. 5). In the statistical analyses, the Akaike information criterion and Schwarz criterion scores were lower for the three-compartment than for the two-compartment model (Table 3). Moreover, F-statistics rejected the null hypothesis, i.e., that the two-compartment model more adequately describes radioligand uptake.

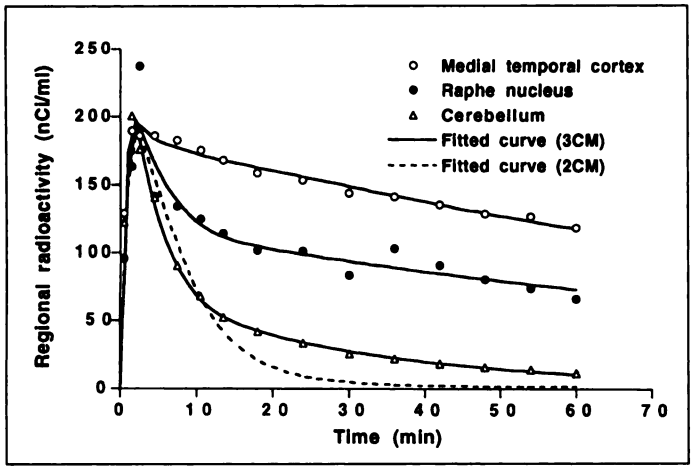

FIGURE 5. Experimental values for regional radioactivity and corresponding fitted curves obtained by three-compartment model in Subject B. Dashed line indicates the fit of two-compartment model to cerebellum.

In the graphical analysis, a linear phase was observed for all regions, including the cerebellum (Fig. 6). The slope of the fitted line is given in Table 1. Theoretically, this slope corresponds to the total volume of distribution, V_t. The linear graphical analysis gave BP values that ranged between 3.3 and 7.9 among the neocortical regions (Table 2).

Assuming that the cerebellum is a valid reference region for free and nonspecifically bound carbonyl-^{11}C-WAY-100635, this region was used as an estimate for $C_n(t)$ to calculate specific binding $C_b(t)$ in ROIs. The time curves for specific binding reached a peak level during time of measurement. As can be seen from Figure 4B, the specific binding was maximal after 20–30 min, thus satisfying a condition for transient equilibrium (*13*). The time of transient equilibrium was calculated from the fitted curves that were obtained in the kinetic analysis. The average time (n = 6) varied between 20 and 25 min for the cortical regions and was 31 min for the raphe (Table 2). The BP, i.e., the $C_b(t)$-to-$C_n(t)$ ratio, varied between 2.6 and 4.7.

The metabolism of carbonyl-^{11}C-WAY-100635 was measured in plasma by HPLC (Fig. 7). The HPLC chromatogram revealed several labeled metabolites. Early peaks (I) represent polar metabolites. One peak (II) comigrated with reference cyclohexanecarboxylic acid and another (IV) with reference desmethyl-WAY-100635. The metabolism was rapid, and the fraction of unchanged carbonyl-^{11}C-WAY-100635 was <10% 10 min after injection in all human subjects (Fig. 8).

DISCUSSION

After intravenous injection of carbonyl-^{11}C-WAY-100635, radioactivity was high in all neocortical regions and the raphe nuclei (Figs. 3 and 4). Radioactivity was highest in the medial temporal lobe, a region that includes the hippocampus. This distribution of radioactivity is in good agreement with autoradiographic studies on the distribution of 5-HT_{1A} receptors in the human brain in vitro using ^{3}H-8-OH-DPAT (*28–30*) or ^{3}H-labeled WAY-100635 (*12*).

The time-activity curves for the neocortex and the raphe nuclei were well described by the three-compartment model (Fig. 5 and Table 1). The forward rate constant k_3 includes the receptor density B_{max} and was highest in the medial temporal cortex, which is in agreement with the known high density of 5-HT_{1A} receptors in this region (*12*). The raphe nuclei is a region of particular interest because the presynaptic 5-HT_{1A} receptor has been given a central role in relation to the treatment of anxiety and depression. The PET system provided a good signal-to-noise ratio for the raphe nuclei. Worth noting, however, is that the coefficient of variance for the rate constants was highest for the raphe nuclei, a variability that probably reflects partial volume effects in relation to the small size of this structure. The raphe nuclei have transaxial extensions of 1–2 mm and extend ~10 mm along the longitudinal axis of the brain stem.

The binding of WAY-100635 is reversible, which is supported by k_4 values above zero. Reversibility of binding was also supported by the linear graphical analysis. The later part of the curves could be described by a linear function, and the slope did not approach infinity (Fig. 6).

The three-compartment model was statistically better than the two-compartment model to describe carbonyl-^{11}C-WAY-100635 binding in the cerebellum (Fig. 5 and Table 3). Two possible explanations are that the second tissue compartment in the cerebellum represents a small amount of specific binding (C_b) or a small amount of kinetically distinguishable nonspecific binding (C_{ns}). The first explanation is not supported by

TABLE 1
Parameters Obtained by Kinetic and Linear Graphical Analysis of Carbonyl-Carbon-11-WAY-100635 Binding

	K_1	k_2	k_3	k_4	V_t	DV^{Logan}
Mean ± s.d. (n = 6)						
Cerebellar cortex	0.17 ± 0.04	0.39 ± 0.05	0.05 ± 0.02[a]	0.05 ± 0.005[b]	0.9 ± 0.2	0.9 ± 0.2
Raphe nucleus	0.14 ± 0.06	0.41 ± 0.24	0.16 ± 0.07	0.02 ± 0.004	4.2 ± 1.6	2.6 ± 0.8
Medial temporal cortex	0.14 ± 0.04	0.30 ± 0.10	0.27 ± 0.06	0.02 ± 0.003	7.6 ± 2.1	8.9 ± 2.0
Lateral temporal cortex	0.15 ± 0.03	0.31 ± 0.06	0.22 ± 0.03	0.02 ± 0.004	5.8 ± 2.3	6.5 ± 2.4
Frontal cortex	0.16 ± 0.04	0.36 ± 0.05	0.19 ± 0.03	0.02 ± 0.002	3.9 ± 1.2	4.3 ± 1.3
Coefficient of variance (%)						
Cerebellar cortex	22	14	35*	11†	23	21
Raphe nucleus	39	60	42	25	38	31
Medial temporal cortex	27	34	21	15	28	22
Lateral temporal cortex	19	19	14	16	40	36
Frontal cortex	27	13	14	8	31	30

*k_5 values.
†k_6 values.

postmortem data, indicating that the cerebellum is almost devoid of 5-HT_{1A} receptors (*12,28*) and 5-HT_{1A} receptor mRNA (*31*). Moreover, a recent PET study in cynomolgus monkeys has shown that pretreatment with high doses of unlabeled WAY-100635 or 8-OH-DPAT could not inhibit carbonyl-^{11}C-WAY-100635 binding in the cerebellum (*14*). Accordingly, it is not likely that the second compartment represents specific binding of 5-HT_{1A} receptors.

The alternative explanation that there is a small amount of kinetically distinguishable nonspecific binding in the cerebellum receives some support from the observation that the k_6 value for the cerebellum was different from the dissociation rate constant (k_4) for the other regions (Table 1). Of interest in this regard is that these observations are consistent with those for ^{11}C-raclopride, another ligand that does not bind specifically in the cerebellum (*13,32*). The existence of kinetically distinguishable nonspecific binding questions the common assumption that the two compartments C_f and C_{ns} equilibrate rapidly to form one effective compartment (*17*).

Radioactive metabolites that pass the blood-brain barrier may also explain the problem to describe radioactivity in the cerebellum using a two-compartment model. Carbonyl-^{11}C-

TABLE 2
Binding Potentials for Carbonyl-Carbon-11-WAY-100635 Binding Calculated by Three Quantitative Approaches

	Kinetic analysis (k_3/k_4)	Linear graphical analysis ($DV_{ROI}/Dv_{cerebellum}$) − 1	Transient equilibrium analysis	
			$C_b(t)/C_n(t)$	Time (min)
Cerebellar cortex	1.0 ± 0.3	NA	NA	NA
Raphe nucleus	9.6 ± 2.6	1.6 ± 0.8	3.1 ± 1.0	31 ± 4
Medial temporal cortex	14.3 ± 3.1	7.9 ± 1.1	4.7 ± 1.1	25 ± 2
Lateral temporal cortex	10.4 ± 2.6	5.4 ± 1.5	3.6 ± 1.1	21 ± 3
Frontal cortex	7.8 ± 0.7	3.3 ± 0.7	2.6 ± 0.6	20 ± 1

Values are mean ± s.d. (n = 6).
NA = not applicable.

TABLE 3
Comparison of the Two- and Three-Component Models for Description of Carbonyl-Carbon-11-WAY-100635 Binding in the Cerebellum of Six Healthy Subjects

Subject		K_1 (ml/ml/min)	k_2 (min^{-1})	k_3 (min^{-1})	k_4 (min^{-1})	RSS	AIC	SC	F statistics
A	2CM	0.22	0.25	—	—	68	63	64	$p < 0.0005$
	3CM	0.24	0.34	0.03	0.04	5	31	33	
B	2CM	0.14	0.20	—	—	67	63	64	$p < 0.0005$
	3CM	0.17	0.35	0.05	0.04	2	20	22	
C	2CM	0.14	0.26	—	—	45	57	59	$p < 0.0005$
	3CM	0.17	0.42	0.04	0.04	5	32	34	
D	2CM	0.13	0.25	—	—	64	62	63	$p < 0.0005$
	3CM	0.16	0.47	0.06	0.05	2	15	18	
E	2CM	0.10	0.21	—	—	32	53	54	$p < 0.0005$
	3CM	0.13	0.43	0.07	0.05	1	2	4	
F	2CM	0.13	0.26	—	—	27	50	51	$p < 0.0005$
	3CM	0.15	0.35	0.03	0.05	2	15	18	

2CM = two-component model; 3CM = three-component model; RSS = residual square sum; AIC = Akaike information criteria; SC = Schwartz criteria.

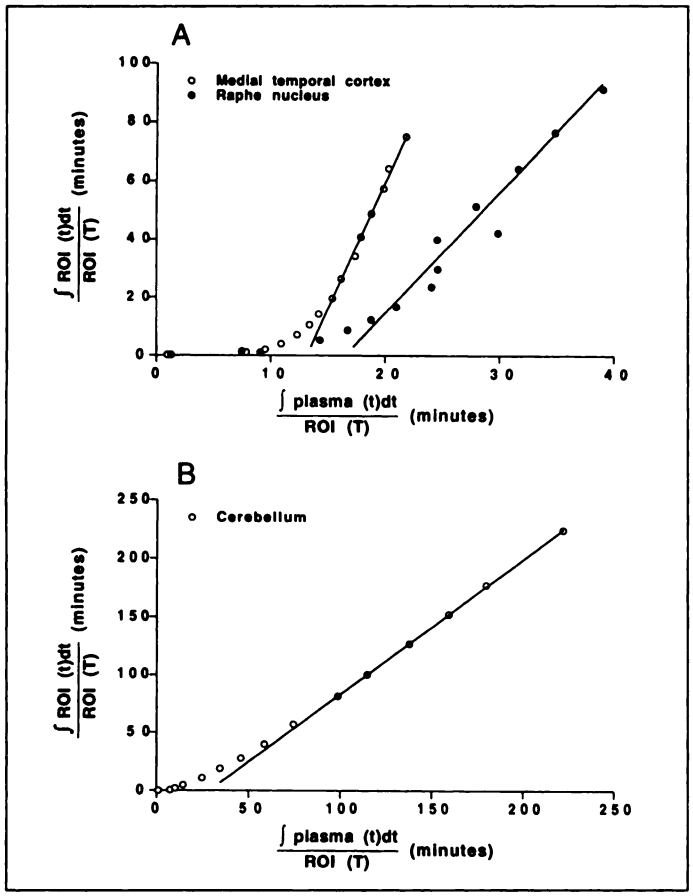

FIGURE 6. Linear graphical analyses of carbonyl-^{11}C-WAY-100635 binding in frontal cortex and raphe (A) and in cerebellum (B) of Subject B.

WAY-100635 was rapidly metabolized (Fig. 8). A very small peak (IV; Fig. 7) had the same chromatographic mobility as desmethyl-WAY-100635. This metabolite has affinity for 5-HT_{1A} receptors in vitro (IC_{50} = 1.4 n*M*; Wyeth Research, *patent data*) and has also been labeled with ^{11}C and shown to bind specifically to 5-HT_{1A} receptors in the monkey brain (*33*). However, the fraction of plasma radioactivity that represents

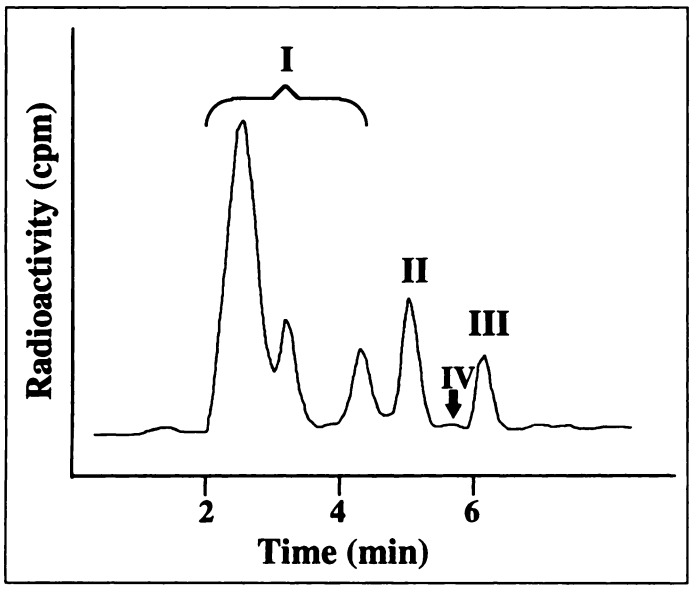

FIGURE 7. Radiochromatogram from gradient HPLC analysis of human plasma at 20 min after intravenous injection of carbonyl-^{11}C-WAY-100635 (Peak III). Peak I, polar-labeled metabolites; Peak II, carbonyl-^{11}C] cyclohexanecarboxylic acid; Peak IV, putative desmethyl-carbonyl-^{11}C-WAY-100635.

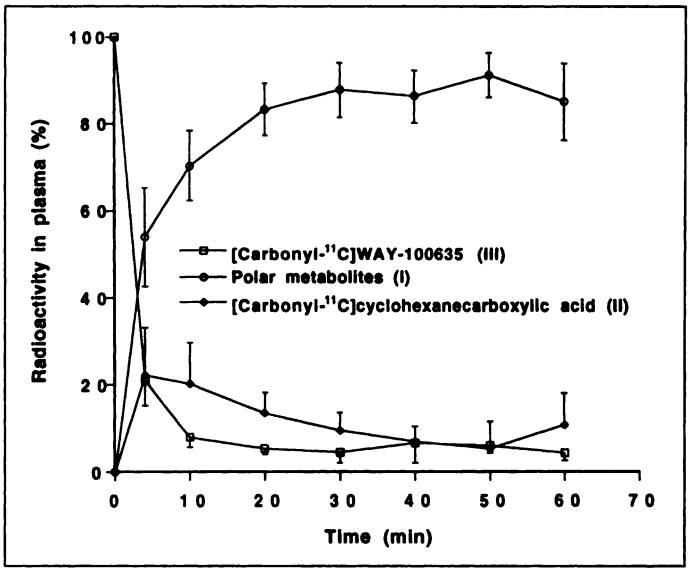

FIGURE 8. Time-activity curves for fraction (%) of radioactivity in plasma that represents unchanged carbonyl-^{11}C-WAY-100635 and two metabolites.

desmethyl-WAY-100635 was, in all cases, <2%. It is, thus, questionable whether this labeled metabolite is of quantitative importance in this analysis of carbonyl-^{11}C-WAY-100635 binding.

The fraction that represents the cyclohexanecarboxylic acid was larger, ~15%. Also this metabolite has recently been labeled with ^{11}C and shown to pass the blood-brain barrier in cynomolgus monkeys (*16*). There was no conspicuous uptake in regions known to contain 5-HT_{1A} receptors, which is consistent with the view that this small molecule has no affinity for 5-HT_{1A} receptors. Importantly, total radioactivity in brain at 2.5 min after injection was 5% for carbonyl-^{11}C-WAY-100635, whereas the corresponding uptake was only 1.2% for carbonyl-^{11}C-cyclohexanecarboxylic acid. This low uptake is consistent with another PET study in monkeys showing that carbonyl-^{11}C-cyclohexanecarboxylic acid contributes to only 8% of the radioactivity at 60 min after injection of carbonyl-^{11}C-WAY-100635 (*34*). Despite this low uptake, it cannot be excluded that carbonyl-^{11}C-cyclohexanecarboxylic acid could contribute to the failure of the two-compartment model to describe the time-activity curves for the cerebellum.

The observation that the three quantitative methods gave different BP values can be related to the failure of the two-compartment model to describe the time-activity curves for the cerebellum (Table 3). The transient equilibrium and the Logan analysis are dependent on the cerebellum as reference region and gave lower BP values than the kinetic analysis. Of the three methods compared, the kinetic analysis should, thus, provide the most valid estimates for the BP.

The transient equilibrium analysis does not require a metabolite-corrected arterial input function and is accordingly simple to use for determination of 5-HT_{1A} receptor occupancy during drug treatment or to obtain BP values in patients with psychiatric disorders. The use of this method for applied studies requires that the identified third compartment in the cerebellum represents unbound radioligand and rapidly equilibrating nonspecific binding. The calculation of receptor occupancy in individual drug-treated patients has often been based on the use of reference values for the BP obtained in control subjects at untreated conditions (*35*). A low interindividual variability of the ratio between radioactivity in the cerebellum and unbound in plasma should, accordingly, be advantageous for reliable

calculations of 5-HT_{1A} receptor occupancy. Studies on larger groups of subjects are required to provide more reliable information on the interindividual variability. Of interest in this regard is that the coefficient of variance for the total distribution volume, V_t, was lower for the cerebellum than for any of the other regions examined (Table 1).

CONCLUSION

Carbonyl-^{11}C-WAY-100635 binding in the human brain can be interpreted using a kinetic analysis with a metabolite-corrected arterial input function. It cannot be excluded that kinetically distinguishable nonspecific binding or the formation of a metabolite that passes the blood-brain barrier may represent components of the radioactivity in the cerebellum. Simplified quantitative methods that are dependent on the cerebellum as reference region are advantageous for clinical studies on central $5HT_{1A}$ receptors. However, before clinical use, the reliability of any simplified method must be confirmed.

ACKNOWLEDGMENTS

The assistance of the members of the Karolinska PET center is gratefully acknowledged. This work was supported by the Swedish Medical Research Council (Grant 09114-0613), the Swedish Natural Science Research Council (Grant K-KU 9973-308), the National Institute of Mental Health (Grant NIMH 41205-11) and the Karolinska Institute.

REFERENCES

1. Baldwin D, Rudge S. The role of serotonin in depression and anxiety. *Int Clin Psychopharmacol* 1995;9:41–45.
2. Berendsen HH. Interactions between 5-hydroxytryptamine receptor subtypes: is a disturbed receptor balance contributing to the symptomatology of depression in humans? *Pharmacol Ther* 1995;66:17–37.
3. Artigas F, Perez V, Alvarez E. Pindolol induces a rapid improvement of depressed patients treated with serotonin reuptake inhibitors. *Arch Gen Psychiatry* 1994;51:248–251.
4. Hashimoto T, Kitamura N, Kajimoto Y, et al. Differential changes in serotonin 5-HT_{1A} and 5-HT_2 receptor binding in patients with chronic schizophrenia. *Psychopharmacology* 1993;112(suppl):S35–S39.
5. Joyce JN, Shane A, Lexow N, Winokur A, Casanova MF, Kleinman JE. Serotonin uptake sites and serotonin receptors are altered in the limbic system of schizophrenics. *Neuropsychopharmacology* 1993;8:315–336.
6. Fletcher A, Bill DJ, Bill SJ, et al. WAY100135: a novel, selective antagonist at presynaptic and postsynaptic 5-HT_{1A} receptors. *Eur J Pharmacol* 1993;237:283–291.
7. Khawaja X, Evans N, Reilly Y, Ennis C, Minchin MCW. Characterisation of the binding of [^{3}H]WAY-100635, a novel 5-HT_{1A} receptor antagonist, to rat brain. *J Neurochem* 1995;64:2716–2726.
8. Mathis CA, Simpson NR, Mahmood K, Kinahan PE, Mintun MA. [^{11}C]WAY 100635: a radioligand for imaging 5-HT_{1A} receptors with positron emission tomography. *Life Sci* 1994;55:403–407.
9. Osman S, Lundkvist C, Pike V, et al. Characterization of the radioactive metabolites of the 5-HT_{1A} receptor radioligand, [O-methyl-^{11}C]WAY-100635 in monkey and human plasma by HPLC: comparison of the behaviour of an identified radioactive metabolite with parent radioligand in monkey using PET. *Nucl Med Biol* 1996;23:627–634.
10. Pike VW, McCarron JA, Lammertsma AA, et al. First delineation of 5-HT_{1A} receptor in human brain with PET and [^{11}C]WAY-100635. *Eur J Pharmacol* 1995;283:R1–R3.
11. Pike VW, McCarron JA, Lammertsma AA, et al. Exquisite delineation of 5-HT_{1A} receptors in human brain with PET and [carbonyl-^{11}C]WAY-100635. *Eur J Pharmacol* 1996;301:R5–R7.
12. Hall H, Lundkvist C, Halldin C, et al. Autoradiographic localization of 5-HT_{1A} receptors in the post-mortem human brain using [^{3}H]WAY-100635 and [^{11}C]WAY-100635. *Brain Res* 1997;745:96–108.
13. Farde L, Ginovart N, Ito H, Lundkvist C, Pike V, McCarron J, Halldin C. PET-characterization of [carbonyl-^{11}C]WAY-100635 binding to 5-HT_{1A} receptors in the primate brain. *Psychopharmacology* 1997;133:196–202.
14. Bergström M, Boëthius J, Eriksson L, Greitz T, Ribbe T, Widén L. Head fixation device for reproducible position alignment in transmission CT and positron emission tomography. *J Comput Assist Tomogr* 1981;5:136–141.
15. Farde L, Eriksson L, Blomqvist G, Halldin C. Kinetic analysis of central [^{11}C]raclopride binding to D_2-dopamine receptors studied by PET: a comparison to the equilibrium analysis. *J Cereb Blood Flow Metab* 1989;9:696–708.
16. Osman S, Lundkvist C, Pike V, et al. Radioactive metabolites in monkey and human plasma from the 5-HT_{1A} receptor radioligand [carbonyl-^{11}C]WAY-100635: advantages in PET for signal contrast in PET as aid to biomathematical modelling. *Nucl Med Biol* 1998;125:215–223.
17. Wong D, Gjedde A, Wagner H Jr. Quantification of neuroreceptors in the living human brain. I. Irreversible binding of ligands. *J Cereb Blood Flow Metab* 1986;6:137–146.
18. Mintun M, Raichle M, Kilbourn M, Wooten G, Welch M. A quantitative model for the *in vivo* assessment of drug binding sites with positron emission tomography. *Ann Neurol* 1984;15:217–227.
19. Huang S, Barrio J, Phelps M. Neuroreceptor assay with positron emission tomography. Equilibrium versus dynamic approaches. *J Cereb Blood Flow Metab* 1986;6:515–521.
20. Marquardt D. An algorithm for least-squares estimation of nonlinear parameters. *J Soc Ind Appl Math* 1963;11:431–441.
21. Akaike H. A new look at the statistical model identification. *IEEE Trans Automat Contr* 1974;19:716–723.
22. Schwartz G. Estimating the dimension of a model. *Ann Stat* 1978;6:461–564.
23. Hawkins R, Phelps M, Huang S-C. Effects of temporal sampling, glucose metabolic rates, and disruptions of the blood–brain barrier on the FDG model with and without a vascular compartment. Studies in human brain tumors with PET. *J Cereb Blood Flow Metab* 1986;6:170–183.
24. Laruelle M, Baldwin R, Rattner Z. SPECT quantification of [^{123}I]iomazenil binding to benzodiazepine receptors in nonhuman primates: I. Kinetic modeling of single bolus experiments. *J Cereb Blood Flow Metab* 1994;14:439–452.
25. Logan J, Wolf A, Shiue C-Y, Fowler J. Kinetic modeling of receptor-ligand binding applied to positron emission tomographic studies with neuroleptic tracers. *J Neurochem* 1987;48:73–83.
26. Koeppe R, Mangner T, Betz A. [^{11}C]aminocyclohexanecarboxylate for the measurement of amino acid uptake and distribution volume in human brain. *J Cereb Blood Flow Metab* 1990;10:727–739.
27. Yamaguchi T, Kanno I, Uemura K. Reduction in regional cerebral metabolic rate of oxygen during human aging. *Stroke* 1986;17:1220–1228.
28. Pazos A, Probst A, Palacios JM. Serotonin receptors in the human brain: III. Autoradiographic mapping of serotonin-1 receptors. *Neuroscience* 1987;21:97–122.
29. Hoyer D, Pazos A, Probst A, Palacios JM. Serotonin receptors in the human brain. I. Characterization and autoradiographic localization of 5-HT_{1A} recognition sites. Apparent absence of 5-HT_{1B} recognition sites. *Brain Res* 1986;376:85–96.
30. Dillon KA, Gross-Isseroff R, Israeli M, Biegon A. Autoradiographic analysis of serotonin 5-HT_{1A} receptor binding in the human brain post mortem: effects of age and alcohol. *Brain Res* 1991;554:56–64.
31. Burnet PWJ, Eastwood SL, Lacey K, Harrison PJ. The distribution of 5-HT_{1A} and 5-HT_{2A} receptor mRNA in human brain. *Brain Res* 1995;676:157–168.
32. Ito H, Hietal J, Blomqvist G, Halldin C, Farde L. Comparison of the transient equilibrium and continuous infusion method for quantitative PET analysis of [^{11}C]raclopride binding. *J Cereb Blood Flow Metab* 1998: in press.
33. Pike V, Halldin C, McCarron J, et al. [Carbonyl-^{11}C]Desmethyl-WAY-100635 (DWAY) is a potent and selective radioligand for central $5HT_{1A}$-receptors in vitro and in vivo? *Eur J Nucl Med* 1998;25:338–346.
34. Carson R, Schmall B, Endres C, et al. Kinetic modelling of the 5-HT1A antagonist [carbonyl-^{11}C]-WAY-100635. *J Cereb Blood Flow Metab* 1997;17(suppl):S327.
35. Farde L, Nordström A-L, Wiesel F-A, Pauli S, Halldin C, Sedvzall G. Positron emission tomography analysis of central D_1- and D_2-dopamine receptor occupancy in patients treated with classical neuroleptics and clozapine. Relation to extrapyramidal side effects. *Arch Gen Psychiatry* 1992;49:538–544.